A&A 521, L14 (2010)
DOI: 10.1051/0004-6361/201015107

Astronomy & Astrophysics
Special feature

Herschel/HIFI: first science highlights

Letter to the Editor

Herschel observations of EXtra-Ordinary Sources (HEXOS): detecting spiral arm clouds by CH absorption lines⋆

S.-L. Qin[1], P. Schilke[1,2], C. Comito[2], T. Möller[1], R. Rolffs[2], H. S. P. Müller[1], A. Belloche[2], K. M. Menten[2], D. C. Lis[3], T. G. Phillips[3], E. A. Bergin[4], T. A. Bell[3], N. R. Crockett[4], G. A. Blake[3], S. Cabrit[5], E. Caux[6,7], C. Ceccarelli[8], J. Cernicharo[9], F. Daniel[9,10], M.-L. Dubernet[11,12], M. Emprechtinger[3], P. Encrenaz[10], E. Falgarone[10], M. Gerin[10], T. F. Giesen[1], J. R. Goicoechea[9], P. F. Goldsmith[13], H. Gupta[13], E. Herbst[14], C. Joblin[6,7], D. Johnstone[15], W. D. Langer[13], S. D. Lord[16], S. Maret[8], P. G. Martin[17], G. J. Melnick[18], P. Morris[13], J. A. Murphy[19], D. A. Neufeld[20], V. Ossenkopf[1,21], L. Pagani[5], J. C. Pearson[13], M. Pérault[10], R. Plume[22], M. Salez[5], S. Schlemmer[1], J. Stutzki[1], N. Trappe[19], F. F. S. van der Tak[21], C. Vastel[6,7], S. Wang[4], H. W. Yorke[13], S. Yu[13], J. Zmuidzinas[3], A. Boogert[16], R. Güsten[2], P. Hartogh[23], N. Honingh[1], A. Karpov[3], J. Kooi[3], J.-M. Krieg[10], R. Schieder[1], M. C. Diez-Gonzalez[24], R. Bachiller[24], J. Martin-Pintado[9], W. Baechtold[25], M. Olberg[26], L. H. Nordh[27], J. L. Gill[13], and G. Chattopadhyay[13]

(Affiliations are available on page 5 of the online edition)

Received 31 May 2010 / Accepted 1 July 2010

ABSTRACT

We have observed CH absorption lines ($J = 3/2, N = 1 \leftarrow J = 1/2, N = 1$) against the continuum source Sgr B2(M) using the *Herschel*/HIFI instrument. With the high spectral resolution and wide velocity coverage provided by HIFI, 31 CH absorption features with different radial velocities and line widths are detected and identified. The narrower line width and lower column density clouds show "spiral arm" cloud characteristics, while the absorption component with the broadest line width and highest column density corresponds to the gas from the Sgr B2 envelope. The observations show that each "spiral arm" harbors multiple velocity components, indicating that the clouds are not uniform and that they have internal structure. This line-of-sight through almost the entire Galaxy offers unique possibilities to study the basic chemistry of simple molecules in diffuse clouds, as a variety of different cloud classes are sampled simultaneously. We find that the linear relationship between CH and H_2 column densities found at lower A_V by UV observations does not continue into the range of higher visual extinction. There, the curve flattens, which probably means that CH is depleted in the denser cores of these clouds.

Key words. ISM: abundances – ISM: molecules

1. Introduction

While physical and chemical conditions of molecular clouds associated with star-forming regions are widely explored by observing various molecular species, much less is known about the chemistry of the bulk of molecular clouds in the spiral arms of our Galaxy. These have mostly been studied only in the CO molecule, with some exceptions. These exceptions consist of clouds that happen to lie along the line-of-sight to a bright Galactic or extragalactic continuum source, and can be observed in absorption. Examples for spiral arm clouds probed by gas absorption are the Sgr B2, W49, W51, and Cas A millimeter continuum sources, where the chemistry was studied mostly through low-energy lines of molecular species (e.g., Greaves & Williams 1994; Greaves & Nyman 1996; Gerin et al. 2010; Menten et al. 2010; Lis et al. 2010; Schilke et al. 2010; Tieftrunk et al. 1994; Wyrowski et al. 2010). Liszt & Lucas (2002) also made important contributions to this field through observations of absorption line clouds against quasars. The observations show that most of the absorption signal arises from diffuse/translucent clouds with low gas density and excitation temperature, suggesting that the ambient ultraviolet field plays a prominent role in determining the chemistry (Lis et al. 2010; Gerin et al. 2010; Neufeld et al. 2010).

Simple linear molecules are fundamental constituents when studying interstellar chemistry, since they are building blocks for more complex species (e.g., Liszt 2009). The very light hydride radical CH (methylidyne) has been observed in diffuse clouds in front of bright OB stars at optical wavelengths and in dark clouds at radio wavelengths, showing that CH column density is linearly correlated with the optical extinction (A_v) for A_v less than 4^m (e.g., Lang & Wilson 1978; Federman 1982; Sheffer et al. 2008). Observations and chemical models also indicate that CH abundance is lower by a factor of 100–1000 in dense clouds and is mainly located in the surface layers of dense clouds (Viala et al. 1979; de Jong et al. 1979; Boland & Dalgarno 1980; Goicoechea et al. 2004; Polehampton et al. 2007) or low column density clouds (Mattila 1986; Magnani et al. 2005).

⋆ *Herschel* is an ESA space observatory with science instruments provided by European-led Principal Investigator consortia and with important participation from NASA.

The prominent Sagittarius B2 star-forming region is very close (~130 pc) to the Galactic center and at a distance of ~8 kpc from the Sun (Reid et al. 2009). The dense cores contained in it, Sgr B2(N) and Sgr B2(M), are well-studied massive star-forming regions. Sgr B2(M) is stronger at submm wavelengths and also less contaminated by emission lines than its neighbor Sgr B2(N) (Goldsmith et al. 1990; Nummelin et al. 1998), making it the target of choice for absorption studies. HIFI, the Heterodyne Instrument for the Far-Infrared (de Graauw et al. 2010) onboard the *Herschel* Space Observatory (Pilbratt et al. 2010) is an ideal instrument for making such observations. In this Letter, we present high spectral-resolution HIFI observations of CH towards Sgr B2(M).

2. Observations

A full spectral scan of Sgr B2(M) in the HIFI band 1a, covering a frequency range from 479.6 to 560.3 GHz was carried out on March 1, 2010, and was pointed at α(J2000) = $17^h47^m20.2^s$ and δ(J2000) = $-28°23'05.0''$, using the dual beam switch (DBS) mode as part of the guaranteed time key program HEXOS: *Herschel*/HIFI observations of EXtra-Ordinary Sources: The Orion and Sagittarius B2 star forming regions (Bergin et al. 2010). The DBS reference beams lie approximately 3′ east and west (i.e. perpendicular to the roughly north-south elongation of Sgr B2). The 1.1 MHz spectral resolution of the wide band spectrometer (WBS) corresponds to a velocity resolution of ~0.6 km s^{-1} over a 4 GHz IF bandwidth. The data have been processed through the standard pipeline released with version 2.9 of HIPE (Ott et al. 2010), including removal of the standing waves, and subsequently exported to FITS format. The double-sideband (DSB) spectra were deconvolved into single-sideband spectra, including the continuum (Comito & Schilke 2002) using the IRAM GILDAS package. The systematic velocity of the source was corrected to the local stand of rest (LSR) frame. Both H and V polarization data were obtained. The data presented here are averages of the two polarizations with equal weighting. The HIFI beam size at 532 GHz is ~37″, with a main beam efficiency of 0.69.

3. Results

The low-frequency radio transitions of CH are between Λ-type doublet states, while spin-rotational as well as rotational transitions fall in the far-infrared and submillimeter bands (Brown & Evenson 1983). Early observations mainly focused on the low-frequency radio and far-infrared lines, the latter with relative low spectral resolution. The lowest spin-rotational transitions of CH at 532.8 and 536.8 GHz were measured in the laboratory by Amano (2000), thus lying in a range of strong atmospheric water absorption, which makes their observation with ground-based telescope impossible. The level populations for the 532.8 and 536.8 GHz transitions are expected to have a low excitation temperature in most clouds, with the possible exception of the Sgr B2 envelope, and thus provide a good measure of the total column density from absorption measurement.

Six hyperfine components of CH in the ground electronic state ($X\ ^2\prod$), $J = 3/2, N = 1 \leftarrow J = 1/2, N = 1$ near 532.8 ($1+ \leftarrow 1-$, $2+ \leftarrow 1-$, and $1+ \leftarrow 0-$), and 536.8 GHz ($2- \leftarrow 1+$, $1- \leftarrow 1+$, and $1- \leftarrow 0+$) are included in the HIFI band 1a observations of Sgr B2(M). The CH spectra near 532.8 and 536.8 GHz obtained with HIFI are presented in Fig. 1, with multiple velocity components seen in absorption. The observations of CH at $J = 3/2, N = 2 \leftarrow J = 1/2, N = 2$ in far-infrared (~2010 GHz) with a velocity resolution of >30 km s^{-1} towards Sgr B2 using the ISO and the Kuiper Airborne Observatory (KAO) 91.4 cm telescope showed absorption centered on 65 km s^{-1} with an unusually large line width of ~200 km s^{-1} (Stacey et al. 1987; Goicoechea et al. 2004; Polehampton et al. 2007), which samples the gas from both the Galactic center and spiral arm clouds along the light of sight. The HIFI CH spectra are spectrally resolved into multiple velocity components with different line intensities and widths. The strong CH absorption at ~64 km s^{-1} with the largest line width clearly corresponds to the envelope of the Sgr B2(M) cloud. In addition to the Sgr B2(M) absorption cloud, the radial velocities of the other absorption components are consistent with those of the spiral arm clouds and kinematic features associated with the Galactic center (e.g., Greaves & Williams 1994; Menten et al. 2010). HIFI observations of H_2O^+ and H_2O in the spiral arm clouds against the Sgr B2(M) continuum show somewhat different spectral profiles than CH (Schilke et al. 2010; Lis et al. 2010). Probably each molecular species samples slightly different regions within various clouds along the line of sight.

Absorption-line column densities can be calculated from the observed line-to-continuum ratio by Gaussian fitting to the lines, if the absorption spectrum comes from a single molecular-species without hyperfine components, as long as the spectrum is not contaminated by emission from other species. We have not identified any strong interfering lines in the velocity range of the 532.8 and 536.8 GHz CH absorption. However, the hyperfine structure of CH makes it difficult to uniquely assign the absorption to distinct velocity components and calculate their column densities. Taking the hyperfine components and contamination from other species into account, and using the LTE approximation, we modeled the CH spectra by employing XCLASS[1] and the automated fitting routine provided by MAGIX[2]. We adopted 2.73 K as rotation temperature for all absorption components, which is questionable only for the Sgr B2 component itself, since the envelope is hot and dense enough to excite CH. A reliable estimate of the CH column density and abundance in this component has to await detailed radiative transfer modeling. Keeping the velocity offsets fixed, we used 31 absorption components and 1 emission component, as for c-C_3H_2 and $H^{13}CO^+$ cases (Menten et al. 2010) for the CH model fitting. We assume that the opacity at any velocity is a sum of contributions from all CH hyperfine components and that the absorbing layers cover the continuum completely. The best fits to the spectra along with the line opacity as a function of velocity are shown in Fig. 1. The column densities and line widths of the 31 absorption components of the best-fit model are given in Table 1. Based on the results of Menten et al. (2010) and Greaves & Williams (1994), the corresponding name of the spiral arm clouds for each velocity component is also given in Table 1.

The column densities range from 2.3×10^{13} to 5.2×10^{14} cm^{-2}. The Sgr B2 cloud (~64 km s^{-1}) has the largest line width and highest column density. Most of the components have column densities of a few times 10^{13} cm^{-2}. The mean column density is 5.4×10^{13} cm^{-2}, excluding Sgr B2(M). This is similar to the *Herschel*/HIFI observations of CH towards the

[1] We made use of the myXCLASS program (https://www.astro.uni-koeln.de/projects/schilke/XCLASS), which accesses the CDMS (Müller et al. 2001; Müller et al. 2005; http://www.cdms.de) and JPL (Pickett et al. 1998; http://spec.jpl.nasa.gov) molecular data bases.

[2] https://www.astro.uni-koeln.de/projects/schilke/MAGIX

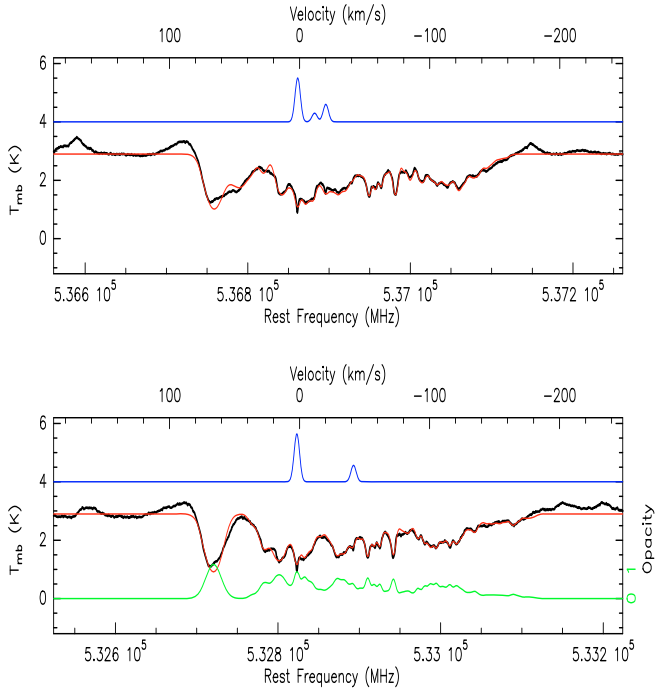

Fig. 1. CH spectra with velocity scale referring to the hyperfine lines at 536.761145 and 532.723926 GHz. *The upper panel* shows the spectrum at 536.8 GHz, *the lower panel* shows the spectrum at 532.8 GHz. The green curve in the bottom panel represents the total opacity as a function of LSR velocity, obtained by linearly adding up the opacities of the hyperfine components. In each panel, the black curve is the observed spectrum, the LTE fit is shown as the red curve, and the blue curve shows the hyperfine pattern for the transition.

massive star-forming region NGC 6334 (Van der Wiel et al. 2010), in which the NGC 6334 envelope has the highest column density of 1.7×10^{14} cm^{-2}, while foreground clouds have a column density of several 10^{13} cm^{-2}. The CH column densities in our observations are similar to those in diffuse clouds and dark nebulae (e.g., Federman 1982; Liszt & Lucas 2002; Mattila 1986). Each spiral arm cloud harbors several velocity components with different line widths and column densities. The velocity structure in each spiral arm cloud suggests that the clouds are not uniform and have internal structure.

4. Discussion

For absorption lines, both the observed antenna temperature and column density of a specific molecule are related to optical depth and excitation temperature. The optical depths in this work are derived from the observed line-to-continuum ratio, therefore the uncertainties due to the absolute flux calibration will not affect the values of the optical depth. The brightness temperature of the background continuum is determined from the baseline offset, which is fairly reliable for HIFI (Bergin et al. 2010). The only assumption is that the absorption completely covers the continuum. The spiral-arm cloud sizes are approximately 3 pc corresponding to 150″ at a distance of 4 kpc (Greaves & Williams 1994), which is more than the size of the Sgr B2(M) continuum. The same set of parameters in the LTE model fits both the spectral features near 532.8 and 536.8 GHz well. The typical optical depths are 0.5, while the largest optical depth is ∼1 at 64 km s^{-1} (see Fig. 1). Thus, our LTE fitting gives a reliable assessment of the column densities.

Table 1. Model-fitting results and abundances.

$V_{\rm lsr}$ (km s^{-1})	ΔV (km s^{-1})	$N_{\rm CH}$ (cm^{-2})	$N_{\rm H_2}{}^a$ (cm^{-2})	$f_{\rm CH}$
64.0^b	13	5.2×10^{14}	5.4×10^{23}	9.6×10^{-10}
38.5^c	6	2.3×10^{13}	1.9×10^{21}	1.2×10^{-8}
32.0^c	7	6.4×10^{13}	6.3×10^{21}	1.0×10^{-8}
22.0^d	7	1.1×10^{14}	3.0×10^{22}	3.8×10^{-9}
17.0^d	5	7.8×10^{13}	2.5×10^{22}	3.2×10^{-9}
12.0^d	5	6.1×10^{13}	2.2×10^{22}	2.8×10^{-8}
8.2^e	4	1.3×10^{14}	2.4×10^{21}	5.4×10^{-8}
2.5^e	5	1.2×10^{14}	1.2×10^{22}	1.0×10^{-8}
–2.5^e	5	9.2×10^{13}	4.8×10^{21}	1.9×10^{-8}
–8.7^e	6	3.9×10^{13}	1.3×10^{21}	3.1×10^{-8}
–15.5^f	6	6.4×10^{13}	2.9×10^{21}	2.2×10^{-8}
–20.0^f	5	6.5×10^{13}	4.3×10^{21}	1.5×10^{-8}
–25.0^f	6	9.7×10^{13}	4.3×10^{21}	2.2×10^{-8}
–29.5^f	4	2.9×10^{13}	2.7×10^{21}	1.1×10^{-8}
–35.5^f	5	2.3×10^{13}	1.2×10^{21}	1.9×10^{-8}
–41.3^f	4	6.9×10^{13}	1.3×10^{21}	5.3×10^{-8}
–45.7^f	4	5.1×10^{13}	4.4×10^{21}	1.2×10^{-8}
–49.0^f	3	4.6×10^{13}	2.3×10^{21}	2.0×10^{-8}
–53.5^f	6	2.9×10^{13}	8.0×10^{20}	3.6×10^{-8}
–58.7^e	4	6.4×10^{13}	2.7×10^{21}	2.4×10^{-8}
–69.8^e	7	4.7×10^{13}	2.0×10^{21}	2.3×10^{-8}
–76.0^e	4	4.1×10^{13}	2.1×10^{21}	2.0×10^{-8}
–80.1^e	4	2.4×10^{13}	9.6×10^{20}	2.5×10^{-8}
–84.3^e	5	5.7×10^{13}	2.1×10^{21}	2.8×10^{-8}
–88.5^e	5	5.1×10^{13}	1.8×10^{21}	2.9×10^{-8}
–93.0^e	5	5.6×10^{13}	2.4×10^{21}	2.3×10^{-8}
–97.5^e	5	4.6×10^{13}	2.4×10^{21}	1.9×10^{-8}
–101.8^e	4	5.9×10^{13}	4.6×10^{21}	1.3×10^{-8}
–106.2^e	5	4.1×10^{13}	2.4×10^{21}	1.7×10^{-8}
–111.6^e	5	2.3×10^{13}	2.2×10^{21}	1.1×10^{-8}
–116.0^e	6	2.4×10^{13}	1.7×10^{21}	1.4×10^{-8}

Notes. [a] The H_2 column densities are decoded from HCO^+ column densities (Menten et al. 2010). [b] Sgr B2(M); [c] Scutum arm; [d] Sagittarius arm; [e] Galactic center; [f] Norma arm (3 and 4 kpc arms).

Determining of the fractional abundance of a molecule relative to H_2 requires the column densities of both the molecules in question and H_2. A direct measurement of H_2 column density is difficult. HCO^+ has been shown to have an approximately constant abundance relative to H_2 in a wide range of environments, including diffuse clouds, low- and high-mass star-forming regions, and compact extragalactic continuum sources (e.g., Greaves & Nyman 1996; Lucas & Liszt 1996; van Dishoeck et al. 1993); therefore, HCO^+ can be taken as a proxy of H_2. However, HCO^+ itself is optically thick in most velocity components. Following Menten et al. (2010), we use the optically thin $H^{13}CO^+$ column densities from Table 4 of Menten et al. (2010) to determine the H_2 column density and fractional abundance of CH relative to H_2 for each velocity component. This procedures takes measured $^{12}C/^{13}C$ ratios in the various spiral-arm clouds into account and assumes a constant HCO^+/H_2 ratio of 5×10^{-9}. The fractional abundances of CH relative to H_2 are listed in the fifth column of Table 2. The derived H_2 column densities range from 1×10^{21} to 3×10^{22} cm $^{-2}$ with a total

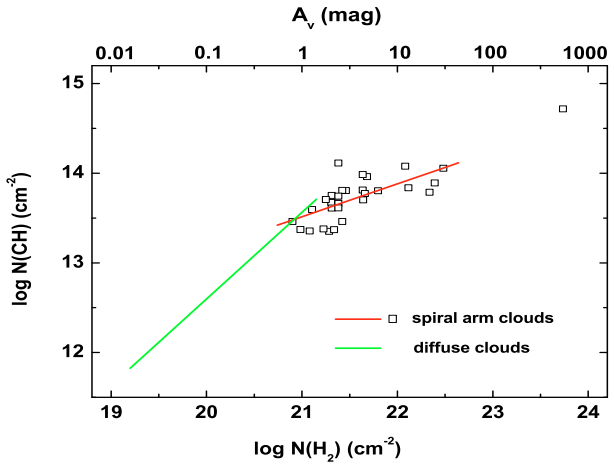

Fig. 2. Correlation of column densities of CH and H_2 in a log-log plot. H_2 column densities are derived from $H^{13}CO^+$ column densities (Menten et al. 2010). The least-squares fit to the data is indicated by the red line. The green line shows the slope of 0.97 fitted to the diffuse clouds in a range of $19.2 < \log N(H_2) < 21.15$ (Sheffer et al. 2008).

column density of 1.6×10^{23} cm $^{-2}$ except for Sgr B2(M), which are roughly consistent with the values derived from ^{13}CO in spiral-arm clouds (Greaves & Nyman 1996; Neufeld et al. 2000). Most of the gas components have a CH fractional abundance of a few times 10^{-8} with an average abundance of 2.1×10^{-8}, excluding the Sgr B2(M) cloud with a value of 9.6×10^{-10} because the excitation there is not straightforward.

Figure 2 presents the relationship between the CH and H_2 column densities. A least-squares fit (excluding the Sgr B2(M) envelope point) gives a slope of $a = 0.38 \pm 0.07$ and an intercept of $b = 5.81 \pm 1.64$ ($\log N(\mathrm{CH}) = a \log N(H_2) + b$) with a correlation coefficient of 0.8. The fits to diffuse clouds ($19 < \log N(H_2) < 21.15$) give a slope of ~1 with a correlation coefficient of 0.99 (Federman 1982; Sheffer et al. 2008), suggesting that N(CH) correlates linearly with $N(H_2)$. In Fig. 2, most of the velocity components in our observations have higher H_2 column densities compared to those of diffuse clouds (Sheffer et al. 2008), and the linear relationship breaks down with $N(H_2) > 10^{21}$ cm^{-1}, i.e. at visual extinctions beyond 1^m, where has a flatter slope of 0.38. The observations of CH and H_2CO towards a few dense molecular clouds associated with massive star formation regions (Genzel et al. 1979) have shown that $N(\mathrm{CH})/N(H_2CO)$ decreases with increasing H_2CO column density, suggesting that CH abundance is lower in dense clouds. The relatively flat slope at higher H_2 column densities and corresponding lower fractional abundances in our observations corraborate the evidence that CH abundance is lower in the inner part of the clouds and predominantly traces lower density environments. As a word of caution, we note that this hinges on the assumption of constant abundance of HCO^+ and has to be tested with other tracers for H_2 column densities.

Previous observations have also shown that the CH column density in photo-dissociation regions (PDR) is not consistent with the linear relationship (Sheffer et al. 2008). Our results appear to agree with the predictions of both turbulent dissipation regions (TDR) and PDR models (see Fig. 8 of Godard et al. 2009) with an H_2 volume density less than 200 cm^{-3}. The chemical network suggests that CH, CH^+, CH_2, C, CH_3^+, CH_2^+, C^+, C_2+, etc. are tightly related by chemistry (Godard et al. 2009). Comparing the column densities of all the hydrides and molecular ions in the absorption line clouds, as provided by HIFI, will enable us to investigate the relative contributions of photon dominated and turbulence dominated chemistry, and distinguish PDR and TDR models.

Acknowledgements. HIFI has been designed and built by a consortium of institutes and university departments from across Europe, Canada, and the United States under the leadership of SRON Netherlands Institute for Space Research, Groningen, The Netherlands, and with major contributions from Germany, France, and the US. Consortium members are: Canada: CSA, U.Waterloo; France: CESR, LAB, LERMA, IRAM; Germany: KOSMA, MPIfR, MPS; Ireland, NUI Maynooth; Italy: ASI, IFSI-INAF, Osservatorio Astrofisico di Arcetri- INAF; Netherlands: SRON, TUD; Poland: CAMK, CBK; Spain: Observatorio Astronico Nacional (IGN), Centro de Astrobiolog (CSIC-INTA). Sweden: Chalmers University of Technology – MC2, RSS & GARD; Onsala Space Observatory; Swedish National Space Board, Stockholm University – Stockholm Observatory; Switzerland: ETH Zurich, FHNW; USA: Caltech, JPL, NHSC.

References

Amano, T. 2000, ApJ, 531, L61
Bergin, E. A., Phillips, T. G., Comito, C., et al. 2010, A&A, 521, L20
Brown, J. M., & Evenson, K. M. 1983, ApJ, 268, L51
Comito, C., & Schilke, P. 2002, A&A, 395, 357
de Graauw, Th., Helmich, F. P., Phillips, T. G., et al. 2010, A&A, 518, L6
de Jong, T., Boland, W., & Dalgarno, A. 1980, A&A, 91, 68
Federman, S. R. 1982, ApJ, 257, 125
Genzel, R., Downes, D., Pauls, T., Willson, R. F., Bieging, J., 1979, A&A, 73, 253
Gerin, M., De Luca, M., Black, J., et al. 2010, A&A, 518, L110
Goldsmith, P. F., Lis, D. C., Hills, R., & Lasenby, J. 1990, ApJ, 350, 186
Godard, B., Falgarone, E., & Pineau Des Forets, G. 2009, A&A, 495, 847
Goicoechea, J. R., Rodriguez-Fernández, N. J., & Cernicharo, José, 2004, ApJ, 600, 214
Greaves, J. S., & Nyman, L.-A. 1996, A&A, 305, 950
Greaves, J. S., & Williams, P. G. 1994, A&A, 290, 259
Lang, K. R., & Wilson, R. F. 1978, ApJ, 224, 125
Leung, C. M., Herbst, E., & Huebner, W. F. 1984, ApJS, 56, 231
Lis, D. C., Phillips, T. G., Goldsmith, P. F., et al. 2010, A&A, 521, L26
Liszt, H. S., & Lucas, R. 2002, A&A, 391, 693
Liszt, H. S. 2009, A&A, 508, 783
Lucas, R., & Liszt, H. 1996, A&A, 307, 237
Magnani, L., Lugo, S., & Dame, T. M. 2005, AJ, 130, 2725
Mattila, K. 1986, A&A, 160, 157
Menten, K. M., Wyrowski, F., Belloche, A., et al. 2010, A&A, accepted
Müller, H. S. P., Thorwirth, S., Roth, D. A., & Winnewisser, G. 2001, A&A, 370, L49
Müller, H. S. P., Schlöder, F., Stutzki, J., & Winnewisser, G. 2005, J. Mol. Struct, 742, 215
Neufeld, D. A., Ashby, M. L. N., Bergin, E. A., et al. 2000, ApJ, 539, L111
Neufeld, D. A., Sonnentrucker, P., Phillips, T. G., et al. 2010, A&A, 518, L108
Nummelin, A., Bergman, P., Hjalmarson, A., et al. 1998, ApJS, 117, 427
Ott, S., et al. 2010, in Astronomical Data Analysis Software and Systems XIX, ed. Y. Mizumoto, K.-I. Morita, & M. Ohishi, ASP Conf. Ser., in press
Pickett, H. M., Poynter, R. L., Cohen, E. A., et al. 1998, J. Quant. Spectrosc. Radiat. Transfer, 60, 883
Pilbratt, G. L., Riedinger, J. R., Passvogel, T., et al. 2010, A&A, 518, L1
Polehampton, E. T., Baluteau, J., Swinyard, B. M., et al. 2007, MNRAS, 377, 1122
Reid, M. J., Menten, K. M., Zheng, X. W., Brunthaler, A., & Xu, Y. 2009, ApJ, 705, 1548
Schilke, P., Comito, C., Müller, H. S. P., et al. 2010, A&A, 521, L11
Sheffer, Y., Rogers, M., Federman, S. R., et al. 2008, ApJ, 687, 1075
Stacey, G. J., Lugten, J. B., & Genzel, R. 1987, ApJ, 313, 859
Tieftrunk, A., Pineau des Forêts, G., Schilke, P., & Walmsley, C. M. 1994, A&A, 289, 579
Van der Wiel, M. H. D., van der Tak, F. F. S, Lis, D. C., et al. 2010, A&A, 521, L43
van Dishoeck, E. F., Blake, G. A., Draine, B. T., & Lunine, J. I. 1993, in Protostars and planets III, ed. E. H. Levy, & J. I. Lunine (Tucson, AZ: Univ. Arizona Press), 163
Viala, Y. P., Bel, N., & Clavel, J. 1979, A&A, 73, 174
Wyrowski, F., Menten, K. M., Guesten, R., & Belloche, A. 2010, A&A, 518, A26

[1] I. Physikalisches Institut, Universität zu Köln, Zülpicher Str. 77, 50937 Köln, Germany
e-mail: qin@ph1.uni-koeln.de
[2] Max-Planck-Institut für Radioastronomie, Auf dem Hügel 69, 53121 Bonn, Germany
[3] California Institute of Technology, Cahill Center for Astronomy and Astrophysics 301-17, Pasadena, CA 91125, USA
[4] Department of Astronomy, University of Michigan, 500 Church Street, Ann Arbor, MI 48109, USA
[5] LERMA & UMR8112 du CNRS, Observatoire de Paris, 61, Av. de l'Observatoire, 75014 Paris, France
[6] Centre d'étude Spatiale des Rayonnements, Université de Toulouse [UPS], 31062 Toulouse Cedex 9, France
[7] CNRS/INSU, UMR 5187, 9 avenue du Colonel Roche, 31028 Toulouse Cedex 4, France
[8] Laboratoire d'Astrophysique de l'Observatoire de Grenoble, BP 53, 38041 Grenoble, Cedex 9, France
[9] Centro de Astrobiología (CSIC/INTA), Laboratiorio de Astrofísica Molecular, Ctra. de Torrejón a Ajalvir, km 4, 28850 Torrejón de Ardoz, Madrid, Spain
[10] LERMA, CNRS UMR8112, Observatoire de Paris and École Normale Supérieure, 24 rue Lhomond, 75231 Paris Cedex 05, France
[11] LPMAA, UMR7092, Université Pierre et Marie Curie, Paris, France
[12] LUTH, UMR8102, Observatoire de Paris, Meudon, France
[13] Jet Propulsion Laboratory, Caltech, Pasadena, CA 91109, USA
[14] Departments of Physics, Astronomy and Chemistry, Ohio State University, Columbus, OH 43210, USA
[15] National Research Council Canada, Herzberg Institute of Astrophysics, 5071 West Saanich Road, Victoria, BC V9E 2E7, Canada
[16] Infrared Processing and Analysis Center, California Institute of Technology, MS 100-22, Pasadena, CA 91125, USA
[17] Canadian Institute for Theoretical Astrophysics, University of Toronto, 60 St George St, Toronto, ON M5S 3H8, Canada
[18] Harvard-Smithsonian Center for Astrophysics, 60 Garden Street, Cambridge MA 02138, USA
[19] National University of Ireland Maynooth, Ireland
[20] Department of Physics and Astronomy, Johns Hopkins University, 3400 North Charles Street, Baltimor e, MD 21218, USA
[21] SRON Netherlands Institute for Space Research, PO Box 800, 9700 AV, Groningen, The Netherlands
[22] Department of Physics and Astronomy, University of Calgary, 2500 University Drive NW, Calgary, AB T2N 1N4, Canada
[23] MPI für Sonnensystemforschung, 37191 Katlenburg-Lindau, Germany
[24] Observatorio Astronómico Nacional (IGN), Centro Astronómico de Yebes, Apartado 148, 19080 Guadalajara, Spain
[25] Microwave Laboratory, ETH Zurich, 8092 Zurich, Switzerland
[26] Chalmers University of Technology, 412 96 Gteborg, Sweden, Sweden/ SRON Netherlands Institute for Space Research, Landleven 12, 9747 AD Groningen, the Netherlands
[27] Department of Astronomy, Stockholm University, 106 91 Stockholm, Sweden